

ENTANGLEMENT DEGRADATION IN THE PRESENCE OF $(4+n)$ -DIMENSIONAL SCHWARZSCHILD BLACK HOLE

DAEKIL PARK

*Department of Physics, Kyungnam University,
Changwon 631-701, Korea*

*Department of Electronic Engineering,
Kyungnam University, Changwon 631-701, Korea*
dkpark@kyungnam.ac.kr
dkpark@hep.kyungnam.ac.kr

Received 31 October 2012

Revised 16 January 2013

Accepted 4 March 2013

Published 16 April 2013

In this paper, we compute the various bipartite quantum correlations in the presence of the $(4+n)$ -dimensional Schwarzschild black hole. In particular, we focus on the n -dependence of various bosonic bipartite entanglements. For the case between Alice and Rob, where the former is free falling observer and the latter is at the near-horizon region, the quantum correlation is degraded compared to the case in the absence of the black hole. The degradation rate increases with decreasing n . We also compute the physically inaccessible correlations. It is found that there is no creation of quantum correlation between Alice and AntiRob. For the case between Rob and AntiRob the quantum entanglement is created although they are separated in the causally disconnected regions. It is found that contrary to the physically accessible correlation the entanglement between Rob and AntiRob decreases with increasing n .

Keywords: Entanglement degradation; higher-dimensional black hole.

1. Introduction

It is evident that quantum information processes such as quantum teleportation,¹ quantum cryptography,^{2–4} and quantum computer^{5,6} will play crucial role in the future technology. In this reason, much attention is paid, recently, to the quantum entanglement⁷ because it is regarded as a genuine physical resource for the quantum information processing.

Although research into the quantum entanglement has a long history,^{8,9} the study of its properties in the relativistic setting was initiated recently.^{10–28} The main issue in this subject is to understand how a given entanglement is changed in the inertial (see Refs. 13–16 and noninertial (see Refs. 17–28) frames. In the noninertial frame,

degradation of the entanglement occurs, which is related to the well-known Unruh effect.^{29,30} More recently, moreover, the change of the entanglement in the black hole background was also examined.^{31–33}

On the other hand, braneworld scenario,^{34–37} one of the modern cosmology, assumes that our $4d$ space–time universe is embedded in higher-dimensional world. In this reason, the absorption and emission properties of the higher-dimensional black holes were investigated few years ago.^{38–42}

The purpose of this paper is to examine the degradation of the bipartite entanglement in the presence of the $(4 + n)$ -dimensional Schwarzschild black hole. In order to explore the degradation we assume that Alice and Rob share the maximally entangled state initially. After sharing, Rob moves to the near-horizon region while Alice is free falling into the black hole. In this situation, we will compute the entanglement by adopting the negativity⁴³ as an entanglement measure. Our main focus in this paper is to investigate the effect of the extra dimensions n in the entanglement degradation. Of course, the result of Ref. 32 is reproduced when $n = 0$.

The paper is organized as follows. In Sec. 2, we review the space–time geometry of the $(4 + n)$ -dimensional Schwarzschild black hole. For later convenience, we compare the $(4 + n)$ -dimensional Schwarzschild space–time with the Rindler space–time in this section. This comparison enables us to transform our problem into the degradation of entanglement in the noninertial frame, which was studied in Refs. 17–28. In Sec. 3, we discuss on the n -dependence of the entanglement. The correlation between Alice and Rob is generally degraded in the presence of the black hole. It is found that the degradation becomes weaker and weaker with increasing n . For the case between Rob and AntiRob, the quantum correlation, contrary to the physically accessible correlation, decreases with increasing n . In Sec. 4, a brief conclusion is given. In Appendix A, explicit computation of negativity is performed.

2. Space–Time Geometry

The higher-dimensional black hole solutions of the Einstein field equation were discussed in detail in Ref. 44. The explicit expression of the $(4 + n)$ -dimensional Schwarzschild black hole solution in terms of the usual Schwarzschild coordinates is in the following:

$$ds^2 = -h(r)dt^2 + h^{-1}(r)dr^2 + r^2d\Omega_{n+2}^2, \quad (1)$$

where

$$\begin{aligned} h(r) &= 1 - \left(\frac{r_H}{r}\right)^{n+1}, \\ d\Omega_{n+2}^2 &= d\theta_{n+1}^2 + \sin^2\theta_{n+1}(d\theta_n^2 + \sin^2\theta_n(\dots + \sin^2\theta_2(d\theta_1^2 + \sin^2\theta_1d\phi^2)\dots)). \end{aligned} \quad (2)$$

The horizon radius r_H is related to the black hole mass M as following:

$$r_H^{n+1} = \frac{8\Gamma\left(\frac{n+3}{2}\right)}{(n+2)\pi^{\frac{n+1}{2}}} \frac{M}{M_*^{n+2}}, \quad (3)$$

where $M_* = G^{-1/(n+2)}$ is a $(4+n)$ -dimensional Planck mass and G is a Newton constant.

Because of the symmetry of the problem we restrict our attention to the temporal and radial coordinates. Thus, the part of the metric we will analyze is

$$d\ell^2 = -h(r)dt^2 + h^{-1}(r)dr^2. \quad (4)$$

We can write the line-element $d\ell^2$ in terms of the proper time τ of an observer located in $r = r_0$ as follows:

$$d\ell^2 = -\frac{h(r)}{h_0}d\tau^2 + h^{-1}(r)dr^2, \quad (5)$$

where $h_0 \equiv h(r_0)$ and $d\tau = \sqrt{h_0}dt$.

Now, we define a new spatial coordinate z as follows:

$$z^2 = \frac{4r_H^{1-n}}{(1+n)^2} (r^{1+n} - r_H^{1+n}), \quad (6)$$

Then, the profile function $h(r)$ can be written as

$$h(r) = \frac{(\kappa z)^2}{1 + (\kappa z)^2}, \quad (7)$$

where κ is a surface gravity defined by

$$\kappa \equiv \frac{1}{2}h'(r_H) = \frac{1+n}{2r_H}. \quad (8)$$

In terms of z it is easy to show that the line-element $d\ell^2$ becomes

$$d\ell^2 = -\frac{1}{h_0} \frac{(\kappa z)^2}{1 + (\kappa z)^2} d\tau^2 + [1 + (\kappa z)^2]^{(1-n)/(1+n)} dz^2. \quad (9)$$

In the near-horizon region, i.e. $r \sim r_H$, Eq. (9) reduces to

$$d\ell^2 \approx -\left(\frac{\kappa z}{\sqrt{h_0}}\right)^2 d\tau^2 + dz^2. \quad (10)$$

This is just the metric of the Rindler space with the acceleration parameter $\kappa/\sqrt{h_0}$.

In order to discuss on the physical states, we define the Kruskal coordinates

$$\bar{u} = -\kappa^{-1}e^{-\kappa(t-r_*)}, \quad \bar{v} = \kappa^{-1}e^{\kappa(t+r_*)}, \quad (11)$$

where the ‘‘tortoise’’ coordinate r_* is defined by

$$\frac{dr_*}{dr} = h^{-1}(r). \quad (12)$$

In terms of the Kruskal coordinates the line-element $d\ell^2$ becomes

$$d\ell^2 = -h(r)e^{-2\kappa r_*} d\bar{u}d\bar{v}. \quad (13)$$

Since r_* reduces to

$$r_* \sim r_H + \frac{r_H}{n+1} \ln \left| \frac{r}{r_H} - 1 \right|$$

at the near-horizon region, we can re-express $d\ell^2$ in this region as

$$d\ell^2 \sim -(n+1)e^{-(n+1)} d\bar{u} d\bar{v} \quad \bar{u}\bar{v} = -\frac{z^2}{n+1}.$$

As authors in Ref. 32 suggested, there are three regions in this background, in which we can define the different time-like Killing vectors. Thus, one should define the physical vacuum in each region. First vacuum is known as the Hartle–Hawking vacuum $|0\rangle_H$. This is defined by the time-like Killing vector which is proportional to $\partial_{\bar{u}} + \partial_{\bar{v}}$. Second and third vacua are the Boulware vacuum⁴⁵ $|0\rangle_B$ and anti-Boulware vacuum $|0\rangle_{\bar{B}}$, which are defined by the time-like Killing vectors ∂_t and $-\partial_t$, respectively.

Since the metric (10) reduces to the Rindler space metric with the acceleration $\kappa/\sqrt{h_0}$ in the near-horizon region, one can derive the interrelations between these vacua using the Unruh effect.^{29,30} The relations beyond the single-mode approximation were derived in Ref. 46. Corresponding $|0\rangle_H$ to Minkowski vacuum and, $|0\rangle_B$ and $|0\rangle_{\bar{B}}$ to the vacua in the left- and right-wedges of Rindler space, one can derive the following relations:

$$\begin{aligned} |0_\Omega\rangle_H &= \frac{1}{\cosh r} \sum_{n=0}^{\infty} \tanh^n r |n_\Omega\rangle_B |n_\Omega\rangle_{\bar{B}}, \\ |1_\Omega\rangle_H &= \frac{1}{\cosh^2 r} \sum_{n=0}^{\infty} \sqrt{n+1} \tanh^n r [q_L |n_\Omega\rangle_B |(n+1)_\Omega\rangle_{\bar{B}} + q_R |(n+1)_\Omega\rangle_B |n_\Omega\rangle_{\bar{B}}], \end{aligned} \quad (14)$$

where $|q_L|^2 + |q_R|^2 = 1$ and

$$\tanh r = \exp\left(-\frac{\pi\sqrt{h_0}\Omega}{\kappa}\right). \quad (15)$$

In Eq. (14), $|m_\Omega\rangle_F$ means m -particle states of energy Ω , which is constructed by operating the creation operator m times to the vacuum $|0\rangle_F$ with $F = \{H, B, \bar{B}\}$. In the next section, we will use Eq. (14) to analyze the bosonic entanglement degradation in the presence of the black hole (1).

3. Entanglement Degradation

Let us consider a situation that Alice and Rob initially share the maximally entangled state

$$|\psi\rangle_{AR} = \frac{1}{\sqrt{2}} (|00\rangle_H + |11\rangle_H)_{AR} \quad (16)$$

when both are free falling into the black hole. Since $\partial_{\bar{u}} + \partial_{\bar{v}}$ is proportional to the time-like Killing vector for the free falling observer, Eq. (16) is understood to be written as a Hartle–Hawking basis. For simplicity, the energy parameters Ω_A and Ω_R for Alice and Rob are ignored in Eq. (16).

Now, we assume that after sharing $|\psi\rangle_{AR}$, Rob moves to the near-horizon region, i.e. $r = r_0 \sim r_H$. Thus, we restrict ourselves into

$$1 < R_S \equiv \frac{r_0}{r_H} < 1.05 \quad (17)$$

throughout this paper. Therefore, Eq. (15) implies

$$\tanh r = \exp\left(-\frac{\Omega}{2}\sqrt{1 - \frac{1}{R_s^{n+1}}}\right), \quad (18)$$

where $\Omega \equiv 2\pi\Omega_R/\kappa$. In this assumption, Eq. (14) implies that $|\psi\rangle_{AR}$ is changed into

$$|\psi\rangle_{ARR} = \frac{1}{\sqrt{2}} \sum_{n=0}^{\infty} \frac{\tanh^n r}{\cosh^2 r} [\cosh r |0, n, n\rangle + \sqrt{n+1} q_L |1, n, n+1\rangle + \sqrt{n+1} q_R |1, n+1, n\rangle]. \quad (19)$$

In this paper, our main interest is to examine the effect of the extra dimension n in the entanglement degradation. Thus, we will choose $q_R = 1$ for simplicity. Furthermore, as shown in Ref. 17, Eq. (14) with $q_R = 1$ case corresponds to the Unruh transformation within the single-mode approximation.

3.1. Alice–Rob quantum correlations

Now, let us discuss on the entanglement between Alice and Rob. In order to examine the entanglement in the presence of the $(4+n)$ -dimensional black hole, we should compute the bipartite entanglement of a quantum state ρ_{AR} , where the subscript AR stands for Alice and Rob. Although there are a lot of entanglement measures which quantify the bipartite entanglement such as entanglement of formation,⁴⁷ concurrence,⁴⁸ and relative entropy of entanglement,⁴⁹ most of them are very hard to compute mainly due to that fact that ρ_{AR} is a state in qudit system. Therefore, we choose a negativity⁴³ in this paper for tractable computation. The negativity \mathcal{N}_{AR} of ρ_{AR} is defined as

$$\mathcal{N}_{AR} = \frac{1}{2} \sum_i (|\lambda_i| - \lambda_i) = - \sum_{\lambda_i < 0} \lambda_i, \quad (20)$$

where λ_i are the eigenvalues of $\rho_{AR}^{T_A}$ and T_A is a partial transposition with respect to the party A . It is worthwhile noting that the negativity \mathcal{N}_{AR} in the absence of the black hole is $1/2$.

The computation of \mathcal{N}_{AR} is described in Appendix A. In Fig. 1, we plot \mathcal{N}_{AR} with varying the number of extra dimensions as $n = 0, 1, 2, 3, 100$. In Fig. 1(a), we

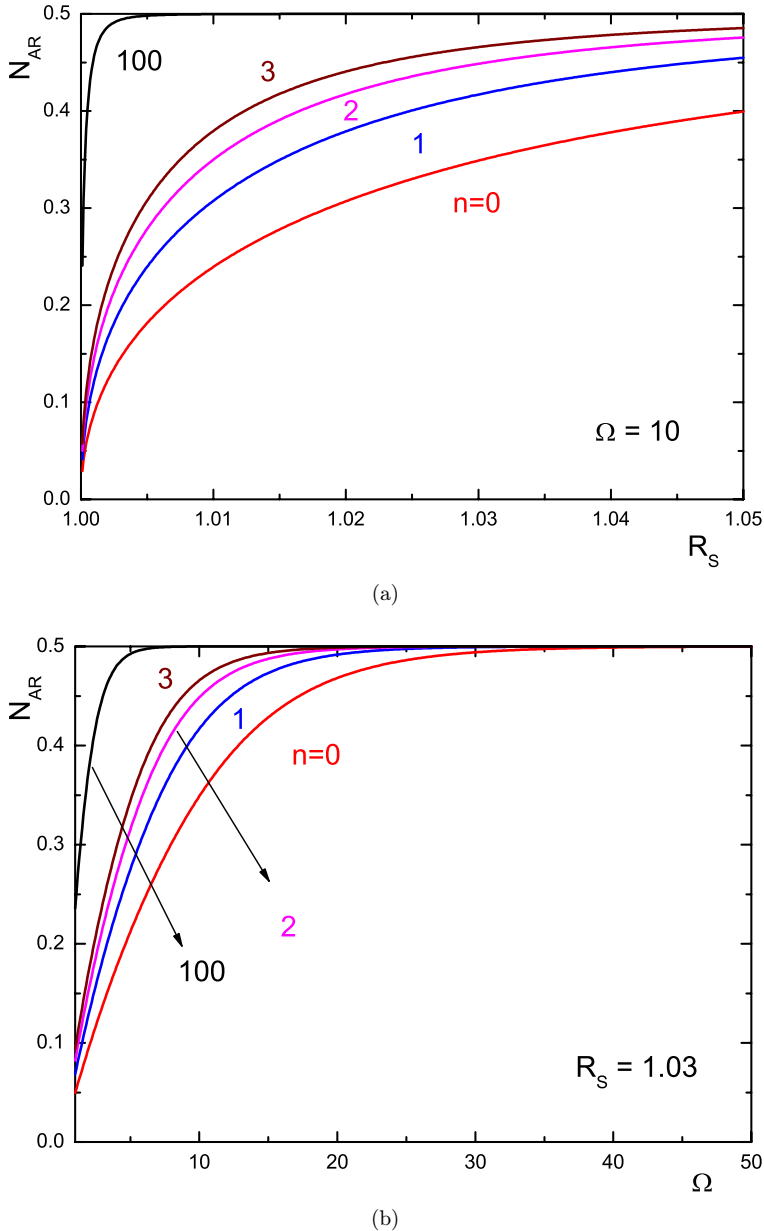


Fig. 1. (Color online) In (a) we plot the R_S -dependence of \mathcal{N}_{AR} when $n = 0, 1, 2, 3, 100$. We fix Ω as $\Omega = 10$. In (b) we plot the Ω -dependence of \mathcal{N}_{AR} when $n = 0, 1, 2, 3, 100$. We fix R_S as $R_S = 1.03$.

plot the R_S -dependence of \mathcal{N}_{AR} with choosing $\Omega = 10$. As this figure exhibits, \mathcal{N}_{AR} is less than 0.5, so that as expected, the degradation of the entanglement occurs. The rate of the degradation decreases with increasing R_S , which means that Rob goes away from the black hole. When Rob approaches to the horizon, i.e. $r_0 \rightarrow r_H$,

all bipartite entanglement vanishes. Another remarkable fact this figure shows is that the degradation becomes weaker with increasing n . This fact can be explained as follows. In $(4+n)$ dimension, the Newtonian gravitational force is proportional to $1/r^{n+2}$. Therefore, it goes weaker and weaker with increasing n . Thus, the effective acceleration Rob needs to remain outside the black hole becomes smaller with increasing n . It causes the weaker degradation of the entanglement between Alice and Rob. In Fig. 1(b), we plot the Ω -dependence of \mathcal{N}_{AR} with choosing $R_S = 1.03$. This figure also shows that the degradation becomes weaker with increasing n . The reason for this fact can be explained the same way.

3.2. Alice–AntiRob quantum correlations

The computation of negativity between Alice and AntiRob is given in Appendix A. It is shown that no entanglement is created between these parties when $q_R = 1$, which corresponds to the Unruh transformation within the single-mode approximation.

3.3. Rob–AntiRob quantum correlations

In Appendix A, the negativity $\mathcal{N}_{R\bar{R}}$ is computed. In Fig. 2, we plot $\mathcal{N}_{R\bar{R}}$ with varying the number of extra dimensions as $n = 0, 1, 2, 3, 10$. In Fig. 2(a), we plot the R_S -dependence of $\mathcal{N}_{R\bar{R}}$ with choosing $\Omega = 10$. In Fig. 2(b), we also plot

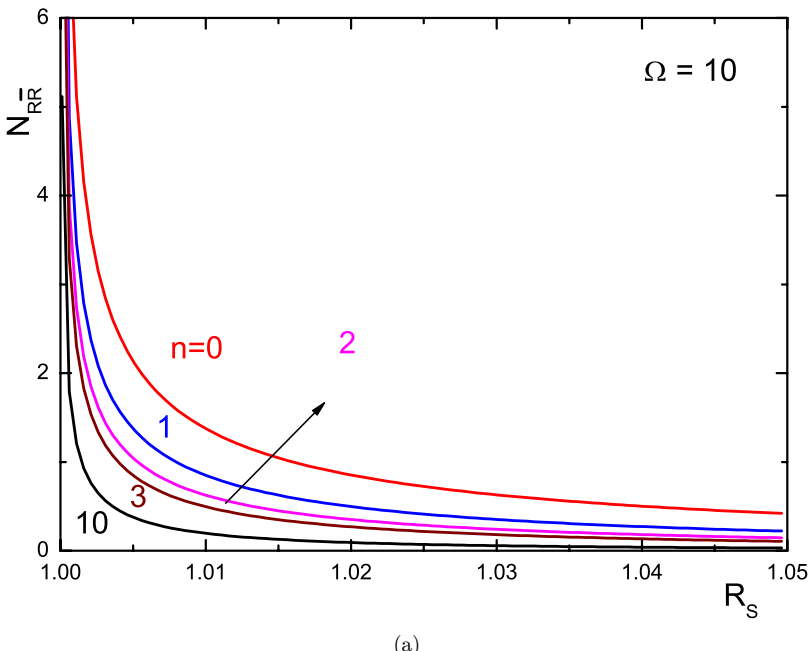


Fig. 2. (Color online) In (a) we plot the R_S -dependence of $\mathcal{N}_{R\bar{R}}$ when $n = 0, 1, 2, 3, 10$. We fix Ω as $\Omega = 10$. In (b) we plot the Ω -dependence of $\mathcal{N}_{R\bar{R}}$ when $n = 0, 1, 2, 3, 10$. We fix R_S as $R_S = 1.03$.

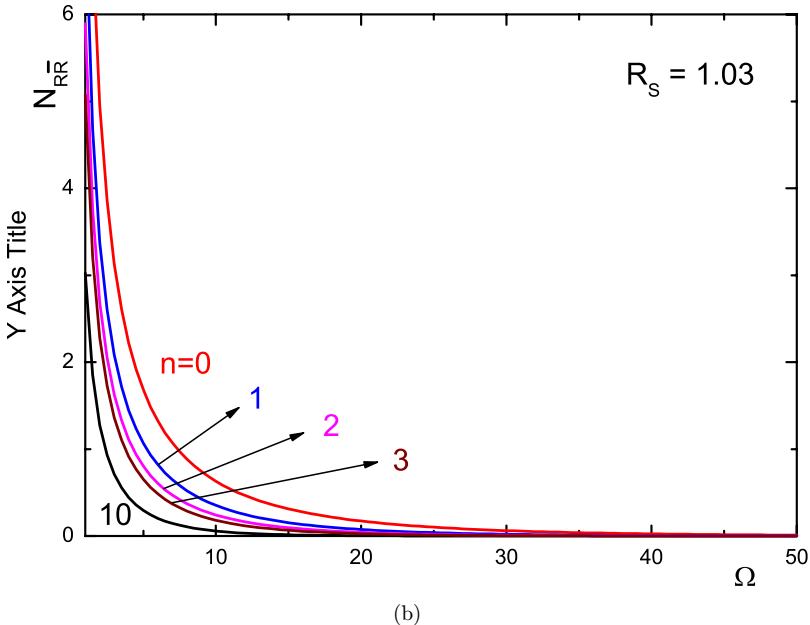


Fig. 2. (Continued)

the Ω -dependence of $\mathcal{N}_{R\bar{R}}$ with choosing $R_S = 1.03$. Contrary to the quantum correlation between Alice and Rob, the quantum entanglement between Rob and AntiRob decreases with increasing n . We do not know why n -dependence of $\mathcal{N}_{R\bar{R}}$ is different from that of \mathcal{N}_{AR} . Probably, this is due to the fact that this entanglement is unphysical because Rob is causally disconnected from AntiRob. Thus, this quantum correlation is purely theoretical and is useless for the quantum information task.

4. Conclusion

In this short paper, we compute the various bipartite quantum correlations in the presence of the $(4+n)$ -dimensional Schwarzschild black hole. In particular, we focus on the n -dependence of the bosonic entanglements. For the case between Alice and Rob the quantum correlation is degraded as expected. The degradation rate increases with decreasing n . However, it is found that there is no creation of quantum correlation between Alice and AntiRob. For the case between Rob and AntiRob, the quantum entanglement is created although they are separated in the causally disconnected regions. The entanglement is found to decrease with decreasing n .

In this paper, we performed the calculation under the condition of $r_0 \sim r_H$. If we relax this condition, various correlations may exhibit different behavior. In this

case, however, we cannot use the Rindler-analogy of the Schwarzschild background. Thus we have to re-derive the equations corresponding to Eq. (14) in this case by computing appropriate Bogoliubov coefficients. However, this generalization might be a difficult problem mainly due to the difficulty in the analytic computation of the Bogoliubov coefficients.

It seems to be of interest to extend this paper to the higher-dimensional rotating black hole case.^{41,42} The condition for occurring the superradiance in the higher-dimensional rotating black holes was derived in Refs. 50 and 51. It seems to be highly interesting to examine the effect of the superradiance to the entanglement degradation.

Acknowledgment

This work was supported by the Kyungnam University Foundation Grant, 2012.

Appendix A

In this appendix we compute the various bipartite entanglement.

A.1. Alice–Rob quantum correlations

Now, we assume that Rob is in the region where Killing vector is ∂_t . Since, then, Rob cannot access the region whose time-like Killing vector is $-\partial_t$, one should take a partial trace over \bar{R} in Eq. (19). Thus, the resulting quantum state for Alice–Rob system becomes a mixed state in a form

$$\begin{aligned} \rho_{AR} &= \text{Tr}_{\bar{R}} |\psi\rangle_{ARR}\langle\psi| \\ &= \frac{1}{2} \sum_{n=0}^{\infty} \frac{\tanh^{2n} r}{\cosh^4 r} [\cosh^2 r |0, n\rangle\langle 0, n| \\ &\quad + (n+1)\{|q_L|^2 |1, n\rangle\langle 1, n| + |q_R|^2 |1, n+1\rangle\langle 1, n+1|\} \\ &\quad + \sqrt{n+1} \cosh r \{q_R |1, n+1\rangle\langle 0, n| + q_R^* |0, n\rangle\langle 1, n+1|\} \\ &\quad + \sqrt{n+1} \sinh r \{q_L |1, n\rangle\langle 0, n+1| + q_L^* |0, n+1\rangle\langle 1, n|\} \\ &\quad + \sqrt{(n+1)(n+2)} \tanh r \{q_L q_R^* |1, n\rangle\langle 1, n+2| \\ &\quad + q_L^* q_R |1, n+2\rangle\langle 1, n|\}]. \end{aligned} \quad (\text{A.1})$$

For $q_R = 1$, computation of \mathcal{N}_{AR} is straightforward from Eq. (A.1). Since $\rho_{AR}^{T_A}$ can be diagonal in terms of 2×2 matrix if one chooses the order of the basis appropriately, the eigenvalues can be easily computed, which is

$$\left\{ \frac{1}{2 \cosh^2 r}, \Lambda_k^\pm \ (k = 0, 1, 2, \dots) \right\},$$

where

$$\Lambda_k^\pm = \frac{\tanh^{2k-2} r}{4 \cosh^4 r} [(k + \cosh^2 r \tanh^4 r) \pm \sqrt{(k + \cosh^2 r \tanh^4 r)^2 + 4 \cosh^2 r \tanh^4 r}]. \quad (\text{A.2})$$

Since $\Lambda_k^+ > 0$ and $\Lambda_k^- < 0$, the negativity between Alice and Rob becomes

$$\mathcal{N}_{AR} = - \sum_{k=0}^{\infty} \Lambda_k^-. \quad (\text{A.3})$$

The extra-dimensional dependence of \mathcal{N}_{AR} arises from n -dependence of r as Eq. (18) shows.

A.2. Alice–AntiRob quantum correlations

From Eq. (19) with $q_R = 1$ the state for Alice–AntiRob becomes

$$\begin{aligned} \rho_{A\bar{R}} &= \text{Tr}_R |\psi\rangle_{ARR}\langle\psi| \\ &= \frac{1}{2} \sum_{n=0}^{\infty} \frac{\tanh^{2n} r}{\cosh^4 r} [\cosh^2 r |0, n\rangle\langle 0, n| + (n+1) |1, n\rangle\langle 1, n| \\ &\quad + \sqrt{n+1} \sinh r \{ |0, n+1\rangle\langle 1, n| + |1, n\rangle\langle 0, n+1| \}]. \end{aligned} \quad (\text{A.4})$$

Since, by similar way, one can show that all eigenvalues of $\rho_{A\bar{R}}^{T_A}$ are positive, we get $\mathcal{N}_{A\bar{R}} = 0$. Thus, no entanglement is created between Alice and AntiRob.

A.3. Rob–AntiRob quantum correlations

From Eq. (19) with $q_R = 1$ the state for Rob–AntiRob becomes

$$\begin{aligned} \rho_{R\bar{R}} &= \text{Tr}_A |\psi\rangle_{ARR}\langle\psi| \\ &= \frac{1}{2} \sum_{m,n=0}^{\infty} \frac{\tanh^{m+n} r}{\cosh^4 r} [\cosh^2 r |n, n\rangle\langle m, m| \\ &\quad + \sqrt{(m+1)(n+1)} |n+1, n\rangle\langle m+1, m|]. \end{aligned} \quad (\text{A.5})$$

Since $\rho_{R\bar{R}}^{T_B}$ is block-diagonal in terms of $m \times m$ ($m = 1, 2, 3, \dots$) matrix provided that the order of the basis is selected as

$$\{|00\rangle, |01\rangle, |10\rangle, |02\rangle, |11\rangle, |20\rangle, \dots\},$$

one can compute the eigenvalues in principle. Therefore, it is possible to compute $\mathcal{N}_{R\bar{R}}$ numerically by making use of Eq. (20).

References

1. C. H. Bennett, G. Brassard, C. Crépeau, R. Jozsa, A. Peres and W. K. Wootters, *Phys. Rev. Lett.* **70** (1993) 1895.
2. C. H. Bennett and G. Brassard, Quantum cryptography: Public key distribution and coin testing, in *Proc. IEEE Int. Conf. Computer, Systems, and Signal Processing*, Bangalore, India (IEEE, New York, 1984), pp. 175–179.
3. A. K. Ekert, *Phys. Rev. Lett.* **67** (1991) 661.
4. C. A. Fuchs, N. Gisin, R. B. Griffiths, C. S. Niu and A. Peres, *Phys. Rev. A* **56** (1997) 1163 [quant-ph/9701039].
5. G. Vidal, *Phys. Rev. Lett.* **91** (2003) 147902 [quant-ph/0301063].
6. M. A. Nielsen and I. L. Chuang, *Quantum Computation and Quantum Information* (Cambridge University Press, Cambridge, England, 2000).
7. R. Horodecki, P. Horodecki, M. Horodecki and K. Horodecki, *Rev. Mod. Phys.* **81** (2009) 865 [quant-ph/0702225] and references therein.
8. A. Einstein, B. Podolsky and N. Rosen, *Phys. Rev. A* **47** (1935) 777.
9. E. Schrödinger, *Naturwissenschaften* **23** (1935) 807.
10. A. Peres and D. R. Terno, *Rev. Mod. Phys.* **76** (2004) 93 [quant-ph/0212023].
11. A. Peres and D. R. Terno, *Int. J. Quantum Inform.* **1** (2003) 225 [quant-ph/0301065].
12. A. Peres, *Fortsch. Phys.* **52** (2004) 1052 [quant-ph/0405127].
13. M. Czachor, *Phys. Rev. A* **55** (1997) 72 [quant-ph/9609022].
14. A. Peres, P. F. Scudo and R. Terno, *Phys. Rev. Lett.* **88** (2002) 230402 [quant-ph/0203033].
15. P. M. Alsing and G. J. Milburn, *Quantum Inform. Comput.* **2** (2002) 487 [quant-ph/0203051].
16. R. M. Gingrich and C. Adami, *Phys. Rev. Lett.* **89** (2002) 270402 [quant-ph/0205179].
17. I. Fuentes-Schuller and R. B. Mann, *Phys. Rev. Lett.* **95** (2005) 120404 [quant-ph/0410172].
18. Y. Ling, S. He, W. Qiu and H. Zhang, *J. Phys.: Math. Theor. A* **40** (2007) 9025 [quant-ph/0608029].
19. Q. Pan and J. Jing, *Phys. Rev. A* **77** (2008) 024302.
20. A. Datta, *Phys. Rev. A* **80** (2009) 052304.
21. J. Wang, J. Deng and J. Jing, *Phys. Rev. A* **81** (2010) 052120.
22. M. R. Hwang, D. K. Park and E. Jung, *Phys. Rev. A* **83** (2011) 012111.
23. E. Martin-Martinez and I. Fuentes, *Phys. Rev. A* **83** (2011) 052306.
24. M. Montero and E. Martin-Martinez, *Phys. Rev. A* **83** (2011) 062323.
25. M. Montero, J. Leon and E. Martin-Martinez, *Phys. Rev. A* **84** (2011) 042320 [arXiv:1108.1111 (quant-ph)].
26. A. Smith and R. B. Mann, arXiv:1107.4633 (quant-ph).
27. D. K. Park, *J. Phys. A: Math. Theor.* **45** (2012) 415308.
28. M.-R. Hwang, E. Jung and D. Park, *Class. Quantum Grav.* **29** (2012) 224004.
29. W. G. Unruh, *Phys. Rev. D* **14** (1976) 870.
30. N. D. Birrel and P. C. W. Davies, *Quantum Fields in Curved Space* (Cambridge University Press, Cambridge, 1982).
31. Q. Pan and J. Jing, *Phys. Rev. D* **78** (2008) 065015.
32. E. Martín-Martínez, L. J. Garay and J. León, *Phys. Rev. D* **82** (2010) 064006.
33. E. Jung, M.-R. Hwang and D. Park, arXiv:1206.5608 (hep-th).
34. N. Arkani-Hamed, S. Dimopoulos and G. Dvali, *Phys. Lett. B* **429** (1998) 263 [hep-ph/9803315].
35. L. Antoniadis, N. Arkani-Hamed, S. Dimopoulos and G. Dvali, *Phys. Lett. B* **436** (1998) 257 [hep-ph/9804398].

36. L. Randall and R. Sundrum, *Phys. Rev. Lett.* **83** (1999) 3370 [hep-ph/9905221].
37. L. Randall and R. Sundrum, *Phys. Rev. Lett.* **83** (1999) 4690 [hep-th/9906064].
38. C. M. Harris and P. Kanti, *J. High Energ. Phys.* **0310** (2003) 014 [hep-ph/0309054].
39. E. Jung and D. K. Park, *Nucl. Phys. B* **717** (2005) 272 [hep-th/0502002].
40. E. Jung and D. K. Park, *Nucl. Phys. B* **766** (2007) 269 [hep-th/0610089].
41. V. Frolov and D. Stojkovic, *Phys. Rev. D* **67** (2003) 084004 [gr-qc/0211055].
42. E. Jung and D. K. Park, *Nucl. Phys. B* **731** (2005) 171 [hep-th/0506204].
43. G. Vidal and R. F. Werner, *Phys. Rev. A* **65** (2002) 032314 [quant-ph/0102117].
44. R. C. Myers and M. J. Perry, *Ann. Phys.* **172** (1986) 304.
45. D. G. Boulware, *Phys. Rev. D* **11** (1975) 1404.
46. D. E. Bruschi *et al.*, *Phys. Rev. A* **82** (2010) 042332.
47. C. H. Bennett, D. P. DiVincenzo, J. A. Smolin and W. K. Wootters, *Phys. Rev. A* **54** (1996) 3824 [quant-ph/9604024].
48. W. K. Wootters, *Phys. Rev. Lett.* **80** (1998) 2245 [quant-ph/9709029].
49. V. Vedral, M. B. Plenio, M. A. Rippin and P. L. Knight, *Phys. Rev. Lett.* **78** (1997) 2275 [quant-ph/9702027].
50. E. Jung, S. Kim and D. K. Park, *Phys. Lett. B* **615** (2005) 273 [hep-th/0503163].
51. E. Jung, S. Kim and D. K. Park, *Phys. Lett. B* **619** (2005) 347 [hep-th/0504139].